

## Effect of Tower Area Change on the Potential of Solar Tower

Atit Koonsrisuk and Tawit Chitsomboon\*

School of Mechanical Engineering, Institute of Engineering, Suranaree University of Technology, Nakhon Ratchasima, Thailand

**Abstract:** Solar tower is a solar power plant for electricity generation by means of air flow induced through a tall tower. Guided by a theoretical prediction, this paper uses CFD technology to investigate the changes in flow kinetic energy caused by the variation of tower flow area with height. It was found that the tower area change affects the efficiency and mass flow rate through the plant. The divergent tower top leads to augmentations in kinetic energy at the tower base significantly.

**Keywords:** Solar Tower, Solar Chimney, Divergent Top Solar Tower, Convergent Top Solar Tower, Efficiency Enhancement

### 1. INTRODUCTION

Solar tower, originally known as solar chimney, is a solar power plant proposed to generate electricity in large scale by transforming solar energy into mechanical energy. In other words, it is an artificial wind generator, albeit a hot one. The schematic of a typical solar tower power plant is sketched in Fig. 1 wherein solar radiation strikes the transparent roof surface, heating the air underneath as a result of the greenhouse effect. Due to buoyancy effect, the heated air flows up the tower and induces a continuous flow from the perimeter towards the middle of the roof where the tower is located. Shaft energy can be extracted from the thermal and kinetic energy of the flowing air to turn an electrical generator [1].

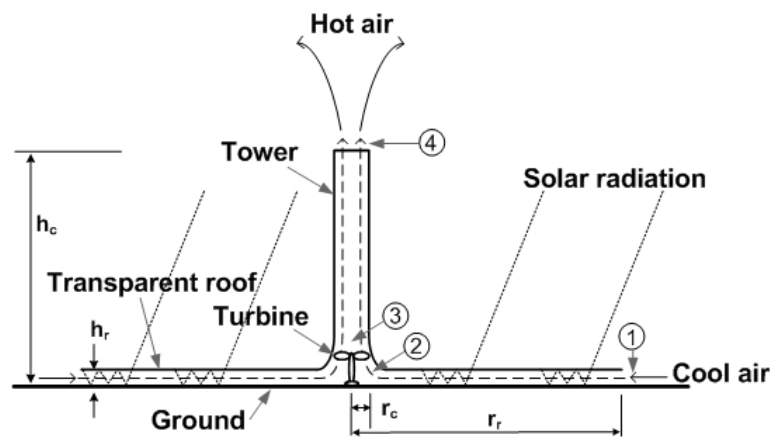


Fig. 1 Schematic layout of straight solar tower power plant

Research works on solar tower started around 1970s, after the construction of a prototype in Manzanares, Spain. The 50 kW prototype produced electricity for seven years, proving that this kind of solar power plant works, although efficiency was rather low [1]. Numerous analytical investigations to predict the flow in solar tower had been proposed [2, 3, 1, 4, 5, 6]. There are common features of all these investigations in that they developed mathematical models from the fundamental equations in fluid mechanics. In doing this the temperature rise due to solar heat gain had been assumed to be reasonable values, using engineering intuition. Flows in the roof and the tower were studied individually without a mechanism to let them interact. Ref. [7] proposed an analytical model with a built-in mechanism through which flows in various parts of a solar tower can naturally interact. Moreover, thermo-mechanical coupling was naturally represented without having to assume an arbitrary temperature rise in the system. The results predicted were compared quite accurately with numerical solutions from Computational Fluid Dynamics (CFD).

The effects of various geometrical parameters on the plant performance were examined by several researchers. Ref. [6] employed a one-dimensional compressible flow model for the calculation of the thermodynamic variables as functions of tower height, wall friction, additional losses, internal drag and tower area change. For a given tower height, an increase in area ratio leads to augmentations in static pressure in the tower. In [4] it was found that efficiency could be increased by tapering the top end of the tower. But in [8] it was found to the contrary that as the tower top is made convergent efficiency does not increase but stays relatively constant.

The present study investigates the influence of tower cross-sectional area changes on the potential of a solar tower power plant. The commercial CFD code "CFX" has been proven to be a reliable tool to simulate the flow in solar tower [9]. To determine the effects of tower profile, the solar tower models with several tower inlet and outlet area ratios were specified and solved by CFX. While [6] and [4] employed one dimensional approach, and [8] used the quasi one dimensional model, the axis-symmetry model is used in this study.

## 2. METHODOLOGY

A theoretical prediction will be examined first in order to guide the present work. The work of [8] proposed a mathematical model for the flow in a solar tower; the results obtained compared very well with CFD results; hence, it will be used as a starting point of this work. The equations was proposed as,

$$\frac{1}{2} \dot{m} v_1^2 \left[ \rho_1 - 2\rho_1 A_1^2 \int_1^3 \frac{dA}{A^3} + \frac{2A_1 \dot{Q}}{v_1 C_p T_1} \int_1^3 \frac{dA_r}{A^2} + \frac{2\rho_1 A_1^2 g h}{\gamma R T_1} \int_1^3 \frac{dA}{A^3} + \rho_1 A_1^2 [A_4^{-2} - A_3^{-2}] \right] = \frac{\rho_1 g h \dot{Q}}{C_p T_3} \int_1^3 dA_r . \quad (1)$$

Numerical subscripts appear in the equation above and equations from here onward are consistent with positions as depicted in Fig. 1. Since the work aim is to evaluate the potential, only a system without a turbine will be analyzed first to reduce the complexity and the added uncertainty that come with the turbine. Therefore, positions 2 and 3 are the same position and will be referred to by the subscript 3.

It is clear from [4, 6, 8] that the important geometrical parameters of the tower are seen to be the tower height,  $h$ , the tower inlet area,  $A_3$ , and the tower outlet area,  $A_4$ . To determine the shape effect of tower, the height and inlet area of tower are fixed, and the outlet area is varied. Hence the study will be focused on convergent-top and divergent-top tower as illustrated in Fig. 2.

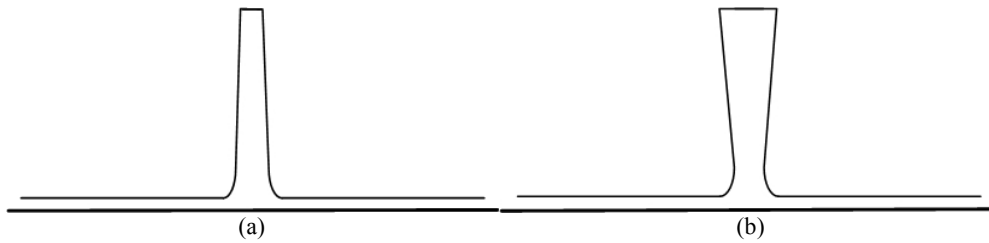


Fig. 2 Schematic layout of (a) convergent-top solar tower; (b) divergent-top solar tower

It can be computed from Eq. (1) that, for a given ambient condition, and fixed  $A_1$  and  $A_3$ , as  $A_4$  increases, the  $\dot{m} v_1^2 / 2$  increases correspondingly. Guided by this mathematical model, it appears that the kinetic energy might increase in proportion to the square of the tower area ratio ( $A_4 / A_3$ ) and this is the main objective of this study. The values of  $A_4 / A_3$  that were used in this study are as listed in Table 1.

Numerical calculations have been performed using CFX. For this purpose, CFX solves the conservation equations for mass, momentum, and energy using a finite volume method. Adaptive unstructured tetrahedral meshes were used in the present study. The plants studied were modeled as an axis-symmetric model where the centerline of the tower is the axis of symmetry. To simulate axis-symmetry, a 5 degree section of the plant is cut out from the entire periphery as shown in Fig. 3.

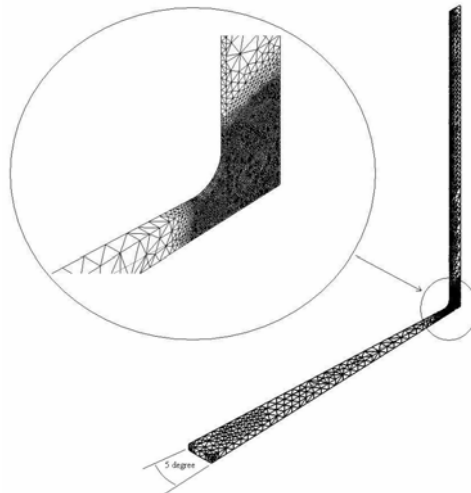


Fig. 3 Unstructured mesh used for the 5 degree axis-symmetric computational domain

Proper boundary conditions are needed for a successful computational work. At the roof inlet, the total pressure and temperature are specified; whereas at the tower exit the 'outlet' condition with zero static pressure is prescribed. The symmetry boundary conditions are applied at the two sides of the sector while the adiabatic free-slip conditions are prescribed to the remaining boundaries, consistent with the frictionless flow assumption. All test cases were computed until residuals of all equations reached their respective minima. Moreover, global conservation of mass were rechecked to further ascertain convergence of the test cases.

**Table 1** Ratio of tower output area to tower input area (AR) and dimensions of plant models

| Case      | AR   | Tower height (m) | Roof height (m) | Roof radius (m) | Tower inlet radius (m) | Tower outlet radius (m) |
|-----------|------|------------------|-----------------|-----------------|------------------------|-------------------------|
| Prototype | 1    | 100              | 2               | 100             | 4                      | 4                       |
| Model 1   | 0.5  | 100              | 2               | 100             | 4                      | 2.83                    |
| Model 2   | 0.75 | 100              | 2               | 100             | 4                      | 3.46                    |
| Model 3   | 2    | 100              | 2               | 100             | 4                      | 5.66                    |
| Model 4   | 4    | 100              | 2               | 100             | 4                      | 8                       |
| Model 5   | 9    | 100              | 2               | 100             | 4                      | 12                      |
| Model 6   | 16   | 100              | 2               | 100             | 4                      | 16                      |

**3. RESULTS AND DISCUSSION**

Figs. 4, 6-8 show the distributions of computed flow properties for different tower area ratio (AR). The abscissa of all plots is the scaled flow path, equaling zero at roof inlet, one at tower top and 0.5 at tower base. As can be seen in Fig. 4 at any AR, the velocity increases as it approaches the tower base. In the tower portion, the velocity distribution depends on AR. For models with AR smaller than one, the velocity keeps on increasing and attains the maximum value at tower outlet. On the other hand, for models with AR larger than one, the flow achieves its maximum velocity right after entering the tower, and then decreases continuously afterward.

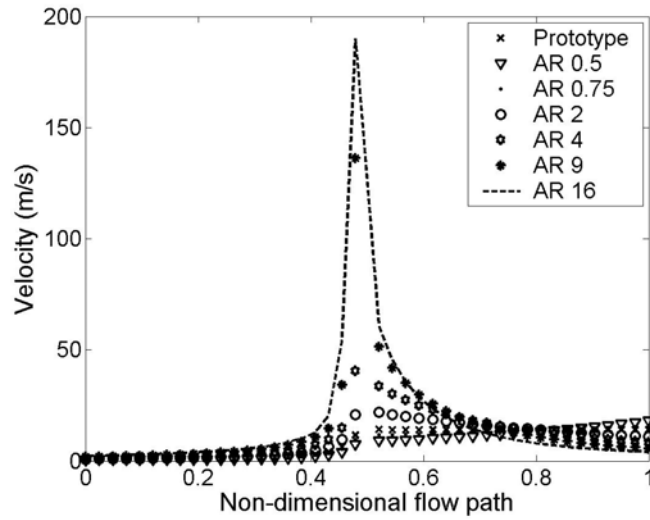


**Fig. 4** Effect of tower area ratio on the velocity profiles for insolation = 800 W/m<sup>2</sup>

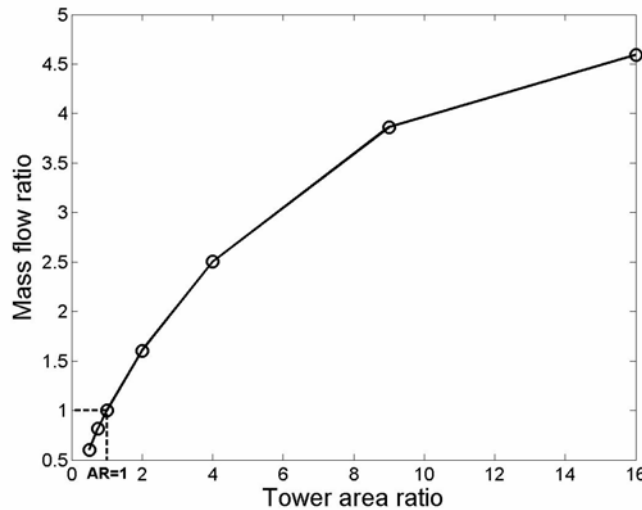


**Fig. 5** Effect of tower area ratio on the mass flow rate for insolation = 800 W/m<sup>2</sup>

The effect of the tower area ratio on the mass flow rate is presented in Fig. 5. The mass flow ratio depicted in Fig. 5 is defined as the ratio of the mass flow rate to the mass flow rate of prototype. The results show that the mass flow rate rises and falls with AR. In relation to the constant-area tower, convergent-top tower reduces mass flow rate and divergent-top tower increases mass flow rate. The temperature, shown in Fig. 6, increases along the flow path in the roof region and remain relatively constant along the tower.

Abrupt dip and rise of the temperature at the tower base is the response to the abrupt velocity change, in accordance with the conservation of energy principle. The noted feature is that the temperature levels in each AR case are widely different, being lower in higher AR cases; this is consistent with the differences in mass flow rates of the various cases as presented in Fig. 5, since a higher mass flow rate should give a lower temperature rise for an equal amount of energy input.

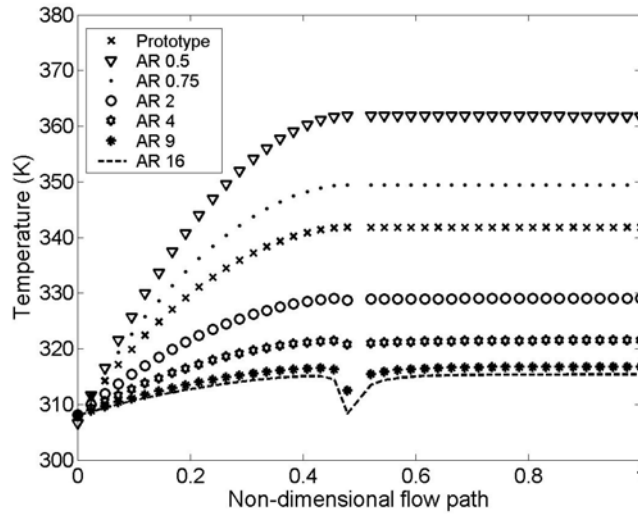


Fig. 6 Effect of tower area ratio on the temperature profiles for insolation = 800 W/m<sup>2</sup>

In Fig. 7, the gauge pressure distributions are seen to be nominally constant under the roof before falling gradually in the tower portion to meet the hydrostatic pressure value at the tower top. For the plants with AR greater than one, there are swift dips at the tower base; the severities of the dips are proportional to AR. The dips are direct responses to the temperature dips because the density is relatively unchanged in a low Mach number flow. Note that the ordinate is the gauge pressure which was scaled such that pressure at the tower top is always zero.

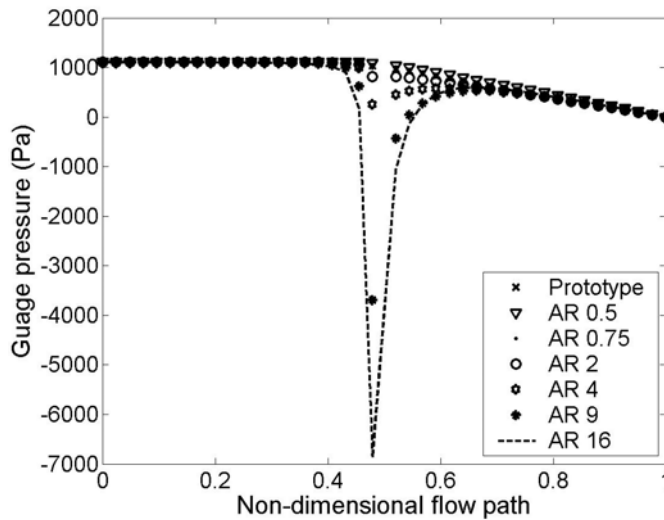
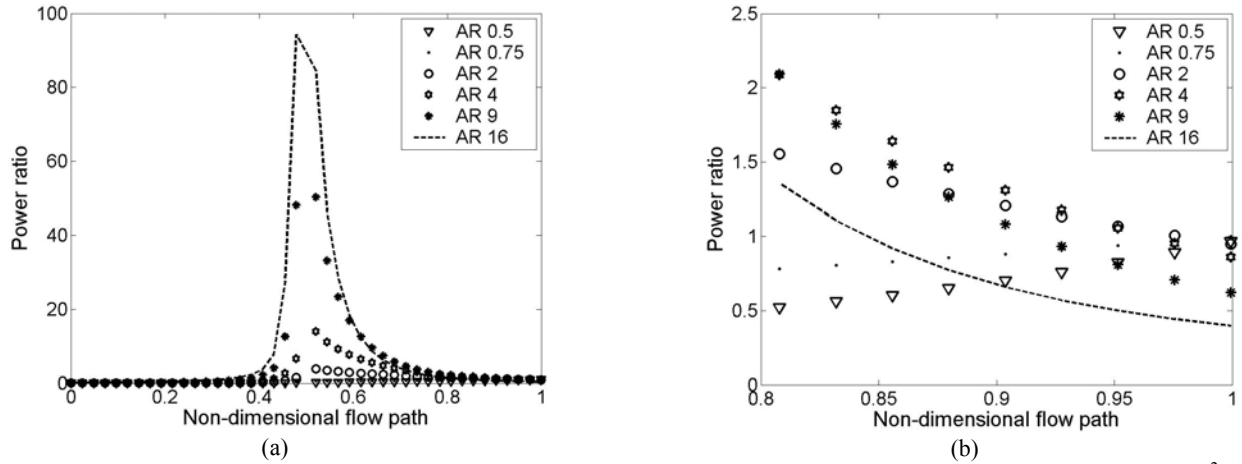


Fig. 7 Effect of tower area ratio on the pressure profiles for insolation = 800 W/m<sup>2</sup>

Fig. 8 shows the variation in dimensionless power, defined as the kinetic power divided by the kinetic energy of the prototype at tower base. It is evident that high AR leads to augmentation in power at the tower base. This suggests the potential of harnessing more turbine power from the high AR system.



**Fig. 8** Effect of tower area ratio on the flow power (scaled by the maximum flow power of prototype) for insolation = 800 W/m<sup>2</sup>: (a) from roof inlet to tower outlet; (b) enlarge view of (a) around tower outlet

Table 2 presents the kinetic energy at the tower base for each model scaled by the prototype kinetic energy at the same location; the square of tower area ratio (AR<sup>2</sup>) of each model is also shown. It is observed that the power increases in proportion to AR<sup>2</sup> when AR ranges between 0.5 to 4 and it increases at a lower rate thereafter. This quadratic trend is suggested by Eq. (1) as mentioned earlier. However, the statement that Eq. (1) suggests a quadratic relation is only on an approximate basis since the equation is implicit and non-linear.

Further inspection of Table 2 shows that the flow kinetic energy and efficiency increase as AR increases. Efficiency in this case is defined as the kinetic energy at tower base divided by the total insolation. This definition is unfair to the convergent top case because its potential is at the top, not at the base. However, Fig. 8 (b) reveals that the kinetic energy at the top of the convergent tower remains the same as the constant area case. So, its potential remains unchanged in relation to the constant area case. This result coincides with that of [8] and contradicts to that of [4].

**Table 2** Kinetic power at the tower base scaled by prototype power, the square of tower area ratio (AR<sup>2</sup>) and the efficiency at tower entrance,  $\eta = 0.5\dot{m}v_3^2 / \dot{Q}A_r$

| Case      | AR   | Power | AR <sup>2</sup> | Efficiency |
|-----------|------|-------|-----------------|------------|
| Prototype | 1    | 1     | 1               | 0.0030     |
| Model 1   | 0.5  | 0.24  | 0.25            | 0.0007     |
| Model 2   | 0.75 | 0.57  | 0.56            | 0.0017     |
| Model 3   | 2    | 3.84  | 4               | 0.0114     |
| Model 4   | 4    | 13.92 | 16              | 0.0414     |
| Model 5   | 9    | 50.26 | 81              | 0.1495     |
| Model 6   | 16   | 94.29 | 256             | 0.2520     |

As shown in Table 2 the efficiency in converting insolation into kinetic energy is rather low, due mainly to the 'shortness' of the tower height. But the increase for the AR=16 case over that of the prototype is quite large, at 94 folds. It would seem that there is an upper bound on AR that can boost up the kinetic energy. Too high AR would eventually lead to boundary layer separation. Friction that comes with high velocity would also reduce the benefit.

#### 4. CONCLUSION

A solar tower system with varying tower flow area has been studied and its performance has been evaluated. The results show that divergent tower helps increase mass flow rate and kinetic energy over that of the constant area tower. The tower area ratio of 16 can produce kinetic energy as much as 94 times that of the constant area tower. For the convergent tower, the velocity at the tower top increases but the mass flow rate decreases in a manner such that the kinetic power at the top remains the same as the constant area case. For the divergent case, maximum kinetic energy occurs at the tower base and this suggests the potential to extract more turbine power than the constant area tower.

#### 5. ACKNOWLEDGMENTS

This research is sponsored by the Royal Golden Jubilee (RGJ) Ph.D. Program of the Thailand Research Fund (TRF).

#### 6. NOMENCLATURE

$A$  flow area, m<sup>2</sup>

|           |  |
|-----------|--|
| $A_r$     | roof area, m <sup>2</sup>                    |
| $C_p$     | specific heat at constant pressure, J/(kg.K) |
| $g$       | gravitational acceleration, m/s <sup>2</sup> |
| $h$       | tower height, m                              |
| $\dot{m}$ | mass flow rate, kg/s                         |
| $\dot{Q}$ | solar heat flux, W/m <sup>2</sup>            |
| $R$       | gas constant, J/kg K                         |
| $T$       | absolute temperature, K                      |
| $v$       | flow velocity, m/s                           |

*Greek symbols*

|          |   |
|----------|---|
| $\gamma$ | specific heats ratio                        |
| $\rho$   | density of working fluid, kg/m <sup>3</sup> |

*Subscripts*

|     |                                     |
|-----|-------------------------------------|
| $1$ | position at roof inlet (Figure 1)   |
| $2$ | position at tower inlet (Figure 1)  |
| $3$ | position at turbine exit (Figure 1) |
| $r$ | roof                                |

## 7. REFERENCES

- [1] Schlaich, J. (1995) *The Solar Chimney: Electricity from the Sun*, Edition Axel Menges, Stuttgart, Germany.
- [2] Haaf, W., Friedrich, K., Mayr, G. and Schlaich, J. (1983) Solar chimneys: part I: principle and construction of the pilot plant in Manzanares, *International Journal of Solar Energy*, **2**,(1), pp 3-20.
- [3] Yan, M.-Q., Sherif, S.A., Kridli, G.T., Lee, S.S. and Padki, M.M. (1991) Thermo-fluid analysis of solar chimneys. *Ind. Applic. Fluid Mech*, ASME FED-2, pp.125-130.
- [4] Padki, M.M. and Sherif, S.A. (1999) On a simple analytical model for solar chimneys, *International Journal of Energy Research*, **23**, pp. 289-294.
- [5] Gannon, A.J. and Von Backström, T.W. (2000) Solar chimney cycle analysis with system loss and solar collector performance, *ASME Journal of Solar Energy Engineering*, **122**, (3), pp 133-137.
- [6] Von Backström, T.W. and Gannon, A.J. (2000) Compressible flow through solar power plant chimneys. *ASME Journal of Solar Energy Engineering*, **122**, (3), pp 138-145.
- [7] Chitsomboon, T. (2001) A validated analytical model for flow in solar chimney. *International Journal of Renewable Energy Engineering*, **3**, (2), pp. 339-346.
- [8] Chitsomboon, T. (1999) The effect of chimney-top convergence on efficiency of a solar chimney. *Proceeding of the 13<sup>th</sup> National Mechanical Engineering Conference*.
- [9] Koonsrisuk, A. and Chitsomboon, T. (2004) Dynamic similarity in model testing of the flow in solar chimney. *Proceeding of the 15<sup>th</sup> International Symposium on Transport Phenomena*.